System-Level Efficiency Optimization of a Linear Induction Motor Drive System

Wei Xu, Dong Hu, Gang Lei, and Jianguo Zhu

***Abstract*—Linear induction motors are superior to rotary induction motors in direct drive systems because they can generate direct forward thrust force independent of mechanical transmission. However, due to the large air gap and cut-open magnetic circuit, their efficiency and power factor are quite low, which limit their application in high power drive systems. To attempt this challenge, this work presents a system-level optimization method for a single-sided linear induction motor drive system. Not only the motor but also the control system is included in the analysis. A system-level optimization method is employed to gain optimal steady-state and dynamic performances. To validate the effectiveness of the proposed optimization method, experimental results on a linear induction motor drive are presented and discussed.**

***Index Terms*—Efficiency optimization control, linear inductor motor, system loss model, system-level optimization.**

I. Introduction

LINEAR induction motors have been applied as traction drives in transportation systems. They have some merits over rotary induction motors (RIMs), such as less mechanical loss and higher acceleration and deceleration. Up to now, there are more than 20 commercial linear metro lines in the world, such as the linear metro in Japan and the Beijing airport rapid transport line in China [1-3].

As a type of linear induction motor, single-sided linear induction motor (SLIM) has been attracted much attention recently. However, the efficiency and power factor of SLIM are generally lower than those of RIM due to the large air gap and cut-open magnetic circuit, which limit its application in high power drive systems. These are two major challenges for the wide application of SLIMs. A lot of research efforts have been directed towards the optimum design of high-efficiency SLIM and its drive for transportation systems [4-7].

There are two popular ways to optimize the performance of SLIM, particularly the efficiency. The first one is the optimum design of SLIM through the investigation of the motor electromagnetic field and the equivalent circuit model (ECM) [1,5]. The second one is the development of optimal control algorithm for SLIM drive, for example, development of efficiency optimization control (EOC) algorithm to improve the efficiency in the operation of SLIM [5-9].

For the motor optimization design, ECM of SLIM is a key issue. The more accurate the ECM is, the better optimization results one can expect to obtain. However, ECM of SLIM is much more complicated than that of RIM due to the large air gap and cut-open magnetic circuit. For the control optimization design, loss model is always required and the control performance highly depends on the accuracy of the loss model. Most loss models include copper loss and core loss only, and do not take the loss of control system into account. Thus, the efficiency improvement is limited.

Apart from the aforementioned problems for the motor and control sides separately, another challenge for the efficiency optimization is the investigation of the whole drive system rather than the motor itself. Motors and controllers are generally integrated into drive systems, such as in-wheel motor and SLIM drive systems. Compared to the optimization of each part, the optimization of the whole drive system is more critical because assembling individually optimized components into a system cannot necessarily ensure an optimal system performance. Thus, a system-level optimization method is required to obtain an optimal SLIM drive system.

Regarding the system level design optimization of electrical drive systems, this is a new and challenging topic in both research and industry because multi-disciplinary analysis and high-dimensional optimization are always involved [10-15]. The effectiveness of the system level optimization method highly depends on the accuracy of the developed model and the efficiency of the employed optimization strategies.

This paper is organized as follows. Section II introduces the ECMs for the SLIM. Section III presents system loss model and an improved EOC strategy for the SLIM. Section IV presents the system-level optimization method for the SLIM drive system. Experimental results for the improved EOC and the system-level optimal scheme are provided in Section V, followed by the conclusion.

II. SLIM Equivalent Circuit Model

Fig. 1 shows a typical SLIM drive structure and system diagram. As shown, the SLIM primary is hanged below the redirector, which is supplied by the inverter on the vehicle. The secondary is flattened on the railway track, which consists of a

This article was submitted for review on 1 May, 2018.

W. Xu and D. Hu are with the School of Electrical and Electronic Engineering, Huazhong University of Science and Technology, Wuhan, China (e-mail: weixu@hust.edu.cn).

G. Lei (the corresponding author) is with the School of Electrical and Data Engineering, University of Technology Sydney, Sydney, 2007, Australia (e-mail: gang.lei@uts.edu.au).

J. Zhu is with the School of Electrical and Information Engineering, The University of Sydney, Australia (e-mail: jianguo.zhu@sydney.edu.au).

copper/aluminium conductive plate and a back iron. Fig. 2 illustrates the structure of an SLIM. As shown, large air gap length and cut-open magnetic circuit are typical characters in SLIM due to the machinery principle. For the analysis of SLIM dynamic model, ECMs are required and presented as follows.

Fig. 3 shows a per-phase ECM of SLIM. In the model, R_s and L_{ls} are the primary resistance and leakage inductance, R_{con} and R_{back} the secondary conductive plate and the back-iron resistances, L_{lr} and L_m the secondary leakage inductance and the magnetizing inductance, respectively. This ECM is developed based on the magnetic equations of the air gap. Among these parameters, the mutual inductance and the secondary resistance are influenced by the edge and end effects greatly, which can be revised by four relative coefficients, K_r, K_x, C_r and C_x to improve the accuracy of the ECM. These four coefficients are obtained based on the using of the equal complex power relationship between the electrical circuit and the magnetic field. The comprehensive derivations of the four coefficients can be found in our previous work [1, 5-7].

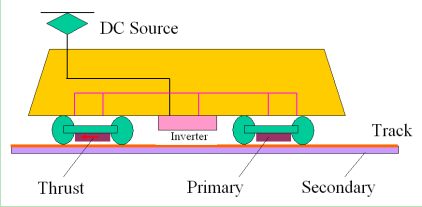

Fig. 1. A diagram of the SLIM drive system.

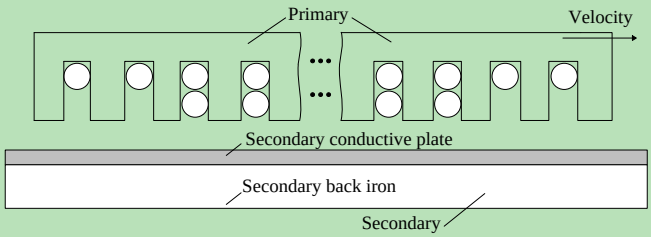

Fig. 2. The structure of SLIM.

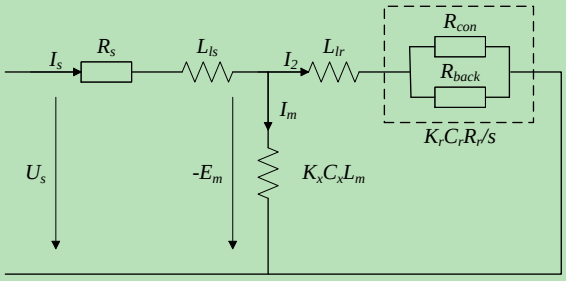

Fig. 3. The per-phase ECM of SLIM.

III. System Loss Model and Improved EOC

A. System Loss Model

There are two major losses in the SLIM drive system, motor and inverter losses. They will be investigated separately and combined into a system loss model.

Firstly, based on secondary field oriented control (FOC) strategy, the secondary flux linkage is oriented to *d*-axis, thus ψ_{qr}=0. Then, the motor losses can be obtained as

$$P_{loss\_SLIM} = a_1\psi_{dr}^2 + a_2 + a_3\psi_{dr}^{-2} + a_4\psi_{dr}^{-4} + a_5\psi_{dr}^{-6} \quad (1)$$

where a_1, a_2, a_3, a_4 and a_5 are the SLIM loss coefficients [6].

Secondly, inverter loss includes conduction loss and switching loss. The inverter losses are obtained as

$$P_{loss\_inv} = n_1 f_1 + n_2 f_1^2 \quad (2)$$

where n_1 and n_2 are the inverter loss coefficients, and f_1 the function of secondary flux linkage, as given by

$$f_1 = \sqrt{\mu_1\psi_{dr}^2 + \mu_2 + \mu_3\psi_{dr}^{-2}} \quad (3)$$

where μ_1, μ_2 and μ_3 are three coefficients [16].

Thirdly, by combing the losses generated by the motor and inverter, the system losses can be calculated by the following equation.

$$P_{loss\_sys} = n_1 f_1 + b_1\psi_{dr}^2 + b_2 + b_3\psi_{dr}^{-2} + a_4\psi_{dr}^{-4} + a_5\psi_{dr}^{-6} \quad (4)$$

where b_1, b_2 and b_3 are three coefficients [6,16].

B. Improved EOC for SLIM Drive

Based on the system loss model, an improved EOC can be developed as shown in Fig. 5. As shown, the total structure is similar to FOC strategy, where thrust force and flux linkage are decoupled. The optimal flux can be obtained by minimizing the system losses of (4). However, it is hard to obtain the analytical solution due to the high-order of the flux linkage. Therefore, the numerical algorithm, Newton- Raphson method, is employed in this work [6].

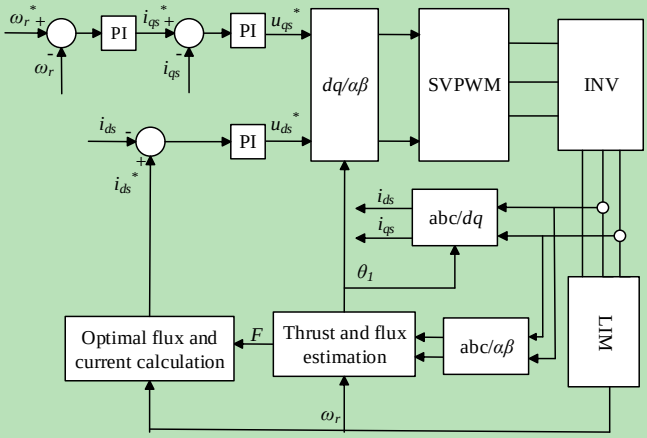

Fig. 4. Diagram of the proposed EOC control strategy.

IV. System-Level Optimization Method

To improve the performances the investigated SLIM and other motor drive systems, optimization is necessary. Many optimization methods have been developed and applied successfully for electrical machines, such as intelligent optimization algorithms, multilevel/sequential optimization methods, and multidisciplinary optimization methods [17-22]. This section will introduce an efficient optimization method for

the investigated SLIM drive system.

A. Optimization Method

A SLIM drive system integrating SLIM and improved EOC control system is studied in this part to illustrate the proposed design optimization method. For the optimization objectives/constraints of this drive system, efficiency, power factor, thrust, output power and dynamic responses of speed and thrust are the main considerations. In this work, fourteen parameters including eight motor parameters as shown in Fig. 5 and six control algorithm parameters as shown in Fig. 4 (PI controller parameters) are included in the optimization.

These parameters are significant to the performance of the system from previous experience. For example, the slip frequency affects the secondary equivalent circuit directly, resulting in big differences in efficiency, power factor, and thrust. For another example, the primary width has significant effects on primary resistance, leakage reactance, and magnetizing reactance. It can change the transversal edge-effect coefficients, too. Fig. 6 illustrates the responses of efficiency, power factor, thrust, and output power in terms of these two design parameters. As shown, all are nonlinear.

There are two popular strategies to solve this kind of high-dimensional system-level optimization problem. The first one is the single-level method, which optimizes all motor and control parameters at the same time. However, this strategy is not efficient for this SLIM drive system. Though the motor optimization is based on the ECM, the dynamic response, such as speed and efficiency are estimated based on the Simulink model in MATLAB, which is time-consuming. For example, if genetic algorithm (GA) or differential evolution algorithm (DEA) is applied, around 14,000 (14*5*200) simulation calls are required for this single-level optimization strategy. Therefore, multi-level optimization strategy is employed in this work to improve the optimization efficiency [17,19-20].

Fig. 7 illustrates the flowchart of the proposed multi-level optimization method for this SLIM drive system. As shown, a three-level optimization structure is proposed, namely motor level, control level, and system level.

Level 1 – Motor level. The aim of this level is to optimize the steady-state performance of the SLIM. Besides, there are also specific physical limitation for the motor design considering the real SLIM in linear metro and the constraints of the laboratory.

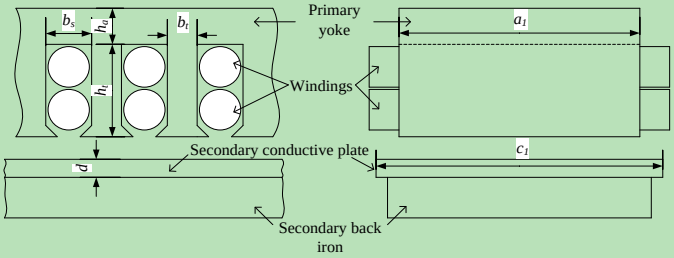

Fig. 5. Optimization parameters illustration of the SLIM.

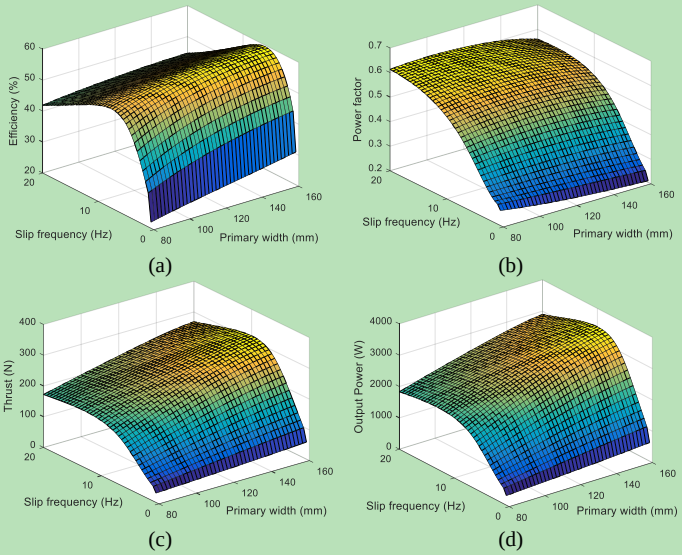

Fig. 6. The primary width and slip frequency and their effects on efficiency (a), power factor (b), thrust (c) and output power (d).

For example, the mechanical air gap is fixed at 10 mm which is the same as real SLIM in linear metro; the primary width and secondary width are bounded up to 150 and 180 mm. respectively; the pole pitch is limited to be smaller than twice of the primary width. In terms of the design specifications, the optimization model is defined as follows.

$$
\begin{aligned}
\max: \quad & f(\mathbf{x}_m) = \eta_m \times \cos\varphi \\
\text{s.t.:} \quad & g_1(\mathbf{x}_m) = \left|P_2 - 3000\right| \le 50, \\
& g_2(\mathbf{x}_m) = J_c - 5.50 \le 0, \\
& g_3(\mathbf{x}_m) = 1.05 - c_1 / a_1 \le 0, \\
& g_4(\mathbf{x}_m) = c_1 / a_1 - 1.50 \le 0, \\
& g_5(\mathbf{x}_m) = \tau - 2a_1 \le 0, \\
& g_6(\mathbf{x}_m) = \left|sf - 0.575\right| \le 0.075, \\
& \mathbf{x}_{ml} \le \mathbf{x}_m \le \mathbf{x}_{mu}
\end{aligned}
\tag{5}
$$

where x_m stands for the motor design parameters, η_m is the motor efficiency, cosφ the power factor, P_2 the output power, and J_c the primary current density. The equations for estimation these performance parameters are based on the impedances of the elements in the per-phase ECM and the complex power [1]. As shown, the main target of this level optimization is to obtain the maximal efficiency and power factor of the SLIM with the limitations/specifications mentioned above. For the implementation of optimization, the DEA is applied as the optimization algorithm to optimize eight structural parameters of SLIM as shown in Fig. 5, based on the per-phase ECM.

Level 2 – Control level. This level aims to optimize both the steady-state and dynamic performances of the control system. A control period including SLIM starting process (FOC) and switching process of the control strategy (from FOC to improved EOC) is investigated and optimized in this level.

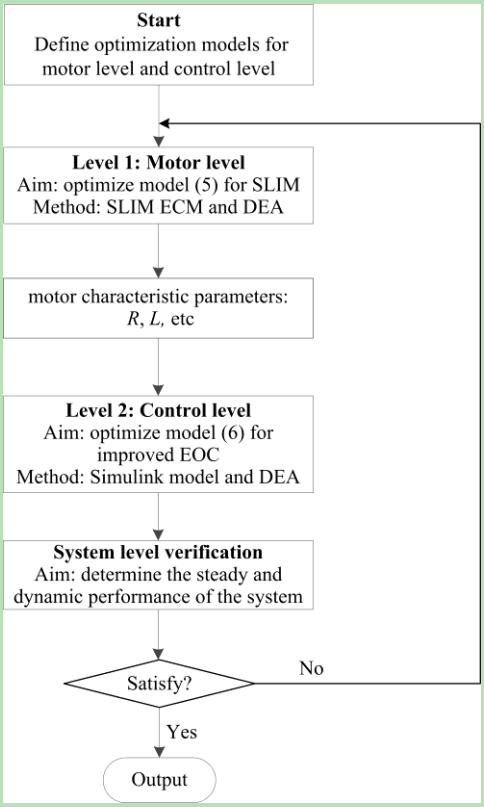

Fig. 7. Multilevel optimization flowchart for the SLIM drive system.

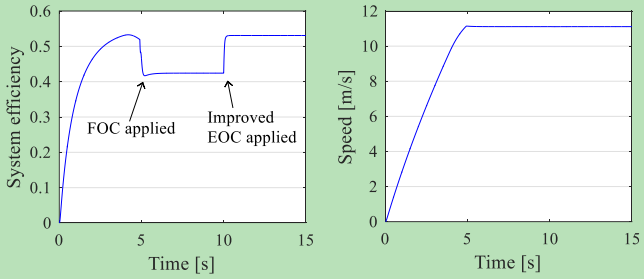

(a) (b)

Fig. 8. System dynamic response after optimization, (a) efficiency, (b) speed.

The objective is to optimize the average efficiency of the drive system with the improved EOC in the steady-state while keeping the dynamic performance of the drive system. The dynamic performance includes the speed overshoot in the starting process and changing processes of the control strategy. The optimization model is defined as

$$\begin{aligned} \max: \quad & f_c(\mathbf{x}_c) = \eta_{system} \\ \text{s.t.:} \quad & g_{c1}(\mathbf{x}_c) = \sigma(\eta_{system}) - 0.005 \le 0, \\ & g_{c2}(\mathbf{x}_c) = \omega_{os} - 0.01 \le 0, \\ & \mathbf{x}_{cl} \le \mathbf{x}_c \le \mathbf{x}_{cu} \end{aligned} \tag{6}$$

where σ means the standard deviation, ω_{os} is speed overshoot. For the optimization, the DEA is applied to optimize six control algorithm parameters based on the Simulink model of the improved EOC as illustrated in Fig. 4.

Level 3 – System level. This level aims to evaluate the system performance and output the optimization results. If the optimal scheme meets the requirements/specifications, end the optimization and output the results, otherwise, return to level 1 and implement the optimization process again.

B. Optimization Results

Fig. 8 shows the dynamic performance including efficiency and speed of the SLIM drive system after optimization. As shown, the system efficiency is increased greatly when the improved EOC is applied. The speed overshoot is quite low for both starting and control switching processes. Meanwhile, as a SLIM will be manufactured as a prototype. Table I lists the optimization results for the motor.

TABLE I
OPTIMIZATION RESULTS OF SLIM

Par.	Description	Unit	Initial	Optimal
h_t	Slot depth	mm	30.5	26.0
b_s	Slot width	mm	10.5	11.2
b_t	Tooth width	mm	5.3	4.4
h_a	Yoke height	mm	35.0	45.0
a_1	Primary width	mm	130.0	130.0
sf	Slip frequency	Hz	10.0	9.8
c_1	SCPW	mm	180.0	180.0
d	SCPT	mm	6.0	5.2
F	Thrust	N	284	277
η	Efficiency	%	48.53	48.74
$cos\varphi$	Power factor	---	0.48	0.52
Obj.	Objective	---	0.23	0.25

V. EXPERIMENTAL VALIDATION

Fig. 9 shows an experimental platform. Experimental results are presented to validate the performances of the proposed improved EOC and the optimized whole drive system. The results are presented as follows.

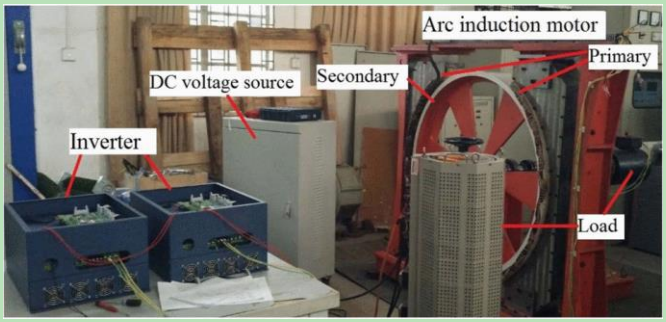

Fig. 9. The experimental platform of the SLIM.

A. Improved EOC

To show the advantages of the improved EOC, two groups of experiments are conducted.

Fig. 10 shows the measured loss and efficiency for FOC and improved EOC under various loads. Due to the limit of the platform (mainly the limit of dc-link voltage), the SLIM is not

able to run at high speed (i.e., 10 m/s) with heavy loads (i.e., more than 50% rated load). Therefore, the test speed is fixed at 5 m/s to obtain the results under various loads. As shown, the losses generated by improved EOC are smaller than those by FOC for all motor, inverter and drive system. Thus, the efficiencies of motor, inverter and drive system have been increased by using improved EOC. Another conclusion can be drawn from this comparison is that the ratio of the decreased system loss is reduced with the increase of the thrust. For example, the system loss can be decreased by 41.04% (275/670) if the thrust is 67 N, while only 2.83% (43/1521) if the thrust is 267 N.

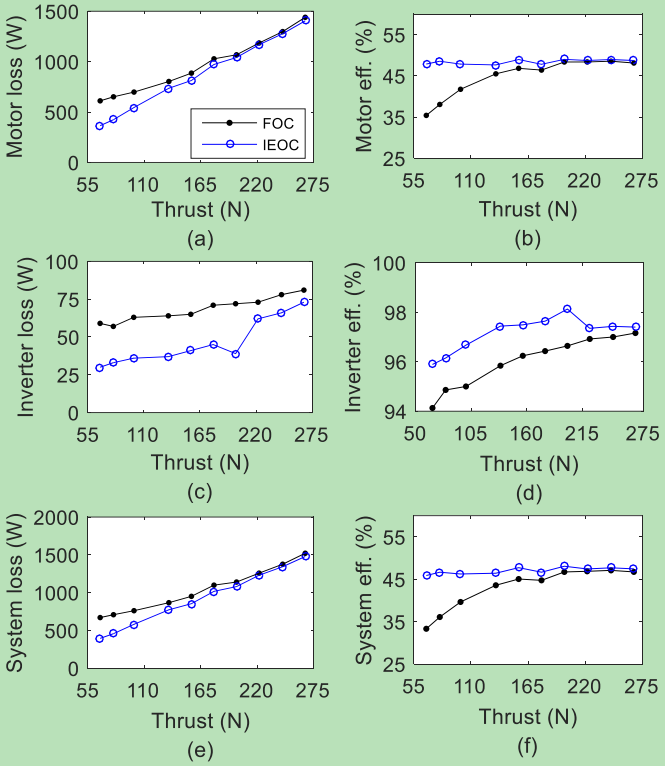

Fig. 10. Measured loss and efficiency for FOC and IEOC under various loads, (a) motor loss, (b) motor efficiency, (c) inverter loss, (d) inverter efficiency, (e) system loss, (f) system efficiency.

Fig. 11 shows the measured loss and efficiency for FOC and improved EOC under various speeds (1-10m/s). In the experiment, a load of 80 N (~30% of full load) is applied to the system. As shown, the loss can be decreased effectively, and the efficiency can be increased greatly (averagely 9.96%) by using the improved EOC.

Based on these comparisons, it can be seen that the improved EOC can effectively increase the efficiency of SLIM drive system. This aligns with the theoretical analysis in section III as well. For the loss model developed based on the equivalent model of SLIM drive, there exists a unique optimal solution to the loss model. Thus, the optimal solution iteratively obtained by the improved EOC method corresponds to the minimal loss, operating point. Consequently, the improved EOC method can increase the SLIM drive efficiency theoretically.

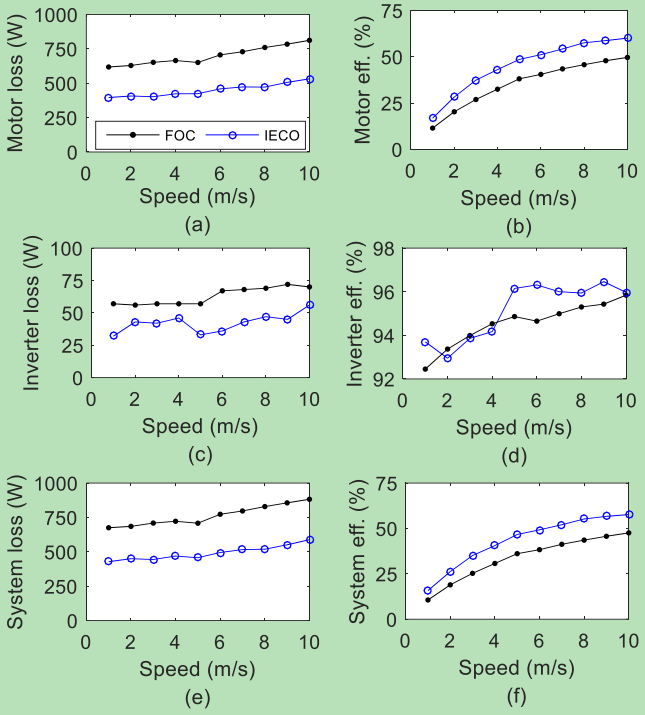

Fig. 11. Measured loss and efficiency for FOC and IEOC under various speeds, (a) motor loss, (b) motor efficiency, (c) inverter loss, (d) inverter efficiency, (e) system loss, (f) system efficiency.

B. Optimal SLIM Drive System

For this experiment, an operation period consisting of two processes is investigated as mentioned in the optimization model. FOC starts at time 5 s under 25% of full load, and then improved EOC applies at 20 s under the same load. Fig. 12 shows the responses of speed and thrust. As shown, the speed overshoot is quite low, meaning good dynamic performance. Fig. 13 illustrates the losses of motor and inverter. As shown, the losses of motor and inverter have been decreased greatly by using improved EOC control method.

Quantitatively, the average losses of motor and inverter in a steady-state period are listed in Table II. As shown, the motor loss has been decreased by 42.62% (from 657 to 377 W), the inverter loss has been decreased by 38.04% (from 92 to 57 W). Based on them, the calculated motor efficiency is increased to 47.05% and inverter efficiency is increased to 92.59% when the improved EOC is applied. The system efficiency is increased to 43.56%, which is a big improvement compared with that of FOC (30.90%). Meanwhile, the inverter efficiency is observed to be optimized slightly compared to the original one. The main reason is that the inverter efficiency is comparatively high, and it is generally difficult to be optimized. Thus, a slight promotion of inverter efficiency is expected to be of great significance for high power SLIM drives.

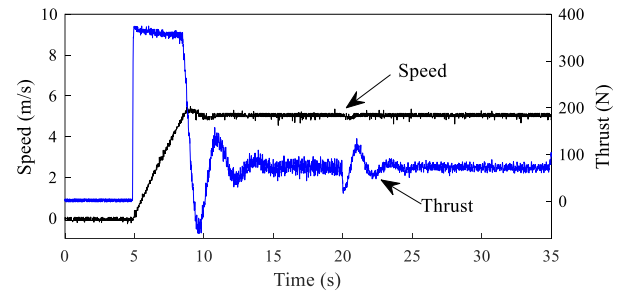

Fig. 12. Dynamic response of speed and thrust for the optimized drive system (with improved EOC applied at time of 20s).

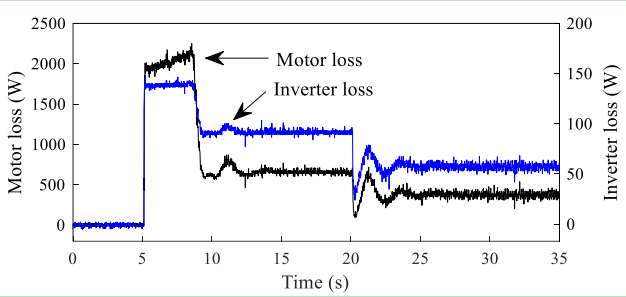

Fig. 13. Losses of SLIM and inverter for the optimized drive system (with improved EOC applied at time of 20s).

TABLE II
COMPARISON OF AVERAGE LOSS AND EFFICIENCY FOR THE OPTIMIZED SLIM DRIVE

Method	Loss (W)		Efficiency (%)	
	Motor	Inv.	Motor	Inv.
FOC	657	92	33.77	91.51
IEOC	377	57	47.05	92.59

VI. CONCLUSION

This work presented a system-level optimization method for a SLIM drive system in metro application. To obtain reliable optimization results, an improved EOC was introduced as the control algorithm based on the system loss model. A multilevel optimization strategy was applied to the drive system optimization to improve the optimization efficiency. Simulation and experimental results were presented to show the efficiency of the proposed method. As shown, the optimal SLIM drive with improved EOC has better steady-state and dynamic performances than driven by the conventional FOC. In addition, the proposed method can be extended to other applications of linear motors.

REFERENCES

[1] W. Xu, J. G. Zhu, *et al.*, "An improved equivalent circuit model of a single-sided linear induction motor," *IEEE Trans. Veh. Technol.*, vol. 59, no. 5, pp. 2277-2289, Jun. 2010.

[2] G. Lv, Z. M. Liu, and S. G. Sun, "Analysis of torques in single-side linear induction motor with transverse asymmetry for linear metro," *IEEE Energy Convers.*, vol. 31, no. 1, pp. 165-173, Jan. 2016.

[3] S. E. Abdollahi, M. Mirzayee, and M. Mirsalim, "Design and analysis of a double-sided linear induction motor for transportation," *IEEE Trans. Magn.*, vol. 51, no. 7, Art. 8106307, Jul. 2015.

[4] E. Amiri and E. A. Mendrela, "A novel equivalent circuit model of linear induction motors considering static and dynamic end effects," *IEEE Trans. Magn.*, vol. 50, no. 3, Art. 8200409, Mar. 2014.

[5] D. Hu, W. Xu, and R. H. Qu, "Electromagnetic design optimization of single-sided linear induction motor for improved drive performance based on linear metro application," in *Proc. IEEE Australasian Universities Power Engineering Conference (AUPEC)*, Sept. 2014, pp. 1-6.

[6] D. Hu, W. Xu, R. J. Dian, Y. Liu, and J. G. Zhu, "Loss minimization control of linear induction motor drive for linear metros, *IEEE Trans. Ind. Electron.*, vol. 65, no. 9, pp. 6870 – 6880, 2018.

[7] D. Hu, W. Xu, G. Lei and J. Zhu, "Design and control optimization of linear induction motor drive for efficiency improvement," 2017 20th International Conference on Electrical Machines and Systems (ICEMS), Sydney, NSW, 2017, pp. 1-6.

[8] Z. Qu, M. Ranta, M. Hinkkanen, and J. Luomi, "Loss-minimizing flux level control of induction motor drives," *IEEE Trans. Ind. Appl.*, vol. 48, no. 3, pp. 952-961, May/Jun. 2012.

[9] Y. Wang, T. Ito, and R. D. Lorenz, "Loss manipulation capabilities of deadbeat direct torque and flux control induction machine drives," *IEEE Trans. Ind. Appl.*, vol. 51, no. 6, pp. 4554-4566, Nov./Dec. 2015.

[10] Gang Lei, Jianguo Zhu, and Youguang Guo, *Multidisciplinary Design Optimization Methods for Electrical Machines and Drive Systems*, Springer-Verlag Berlin Heidelberg, 2016.

[11] G. Lei, J. Zhu, Y. Guo, C. Liu and B. Ma, "A review of design optimization methods for electrical machines", *Energies*, vol. 10, no. 12, Art. no. 1962, pp. 1-31, 2017.

[12] B. Ma, G. Lei, J. Zhu, Y. Guo and C. Liu, "Application-oriented robust design optimization method for batch production of permanent-magnet motors," *IEEE Trans. Ind. Electron.*, vol. 65, no. 2, pp. 1728-1739, 2018.

[13] G. Lei, J. G. Zhu, Y. G. Guo, K. R. Shao and W. Xu, "Multi-objective sequential design optimization of PM-SMC motors for Six Sigma quality manufacturing," *IEEE Trans. Magn.*, vol. 50, no. 2, 2014.

[14] X. Zhu, Z. Xiang, C. Zhang, *et al*., "Co-reduction of torque ripple for outer rotor flux-switching PM motor using systematic multi-level design and control schemes," *IEEE Trans. Ind. Electron.*, vol. 64, no. 2, pp. 1102-1112, 2017.

[15] X. Zhu, Z. Xiang, L. Quan, W. Wu and Y. Du, "Multimode optimization design methodology for a flux-controllable stator permanent magnet memory motor considering driving cycles," *IEEE Trans. Ind. Electron.*, vol. 65, no. 7, pp. 5353-5366, 2018.

[16] L. Aarniovuori, L. I. E. Laurila, M. Niemelä, and J. J. Pyrhönen, "Measurements and simulations of DTC voltage source converter and induction motor losses," *IEEE Trans. Ind. Electron.*, vol. 59, no. 5, pp. 2277-2287, May 2012.

[17] G. Lei, C. C. Liu, J. G. Zhu, and Y. G. Guo, "Techniques for multilevel design optimization of permanent magnet motors," *IEEE Transactions on Energy Conversion*, vol. 30, no. 4, pp. 1574-1584, 2015.

[18] G. Lei, J. G. Zhu, *et al*., "Multi-objective sequential optimization method for the design of industrial electromagnetic devices," *IEEE Trans. Magn.*, vol. 48, no. 11, pp. 4538-4541, 2012.

[19] G. Lei, T. S. Wang, J. G. Zhu, Y. G. Guo, and S. H. Wang, "System level design optimization methods for electrical drive systems: robust approach," *IEEE Trans. Ind. Electron.*, vol. 62, no. 8, pp.4702-4713, 2015.

[20] G. Lei, T. S. Wang, Y. G. Guo, J. G. Zhu, and S. H. Wang, "System level design optimization methods for electrical drive systems: deterministic approach," *IEEE Trans. Ind. Electron.*, vol. 61, no. 12, pp. 6591-6602, 2014.

[21] X. Zhao and S. Niu, "Design and optimization of a new magnetic-geared pole-changing hybrid excitation machine," *IEEE Trans. Ind. Electron.*, vol. 64, no. 12, pp. 9943-9952, Dec. 2017.

[22] Y. Wang, S. Niu and W. Fu, "Sensitivity analysis and optimal design of a dual mechanical port bidirectional flux-modulated machine," *IEEE Trans. Ind. Electron.*, vol. 65, no. 1, pp. 211-220, Jan. 2018.

Wei Xu (M'09-SM'13) received the double B.E. and M.E. degrees from Tianjin University, Tianjin, China, in 2002 and 2005, and the Ph.D. from the Institute of Electrical Engineering, Chinese Academy of Sciences, in 2008, respectively, all in electrical engineering.

From 2008 to 2012, he held several academic positions in both Australian and Japanese universities and companies. Since 2013, he has been full professor with the State Key Laboratory of Advanced Electromagnetic Engineering and Technology, Huazhong University of Science and Technology, China. His research topics mainly cover design and control of linear/rotary machines.

Dong Hu received the B.E. degree in electrical engineering from Huazhong University of Science and Technology, Wuhan, China, in 2013. He is currently working toward the Ph.D. degree at the State Key Laboratory of Advanced Electromagnetic Engineering and Technology, Huazhong University of Science and Technology. His research interests include design and control of linear induction machines.

Gang Lei (M'14) received the B.S. degree in Mathematics from Huanggang Normal University, China, in 2003, the M.S. degree in Mathematics and Ph.D. degree in Electrical Engineering from Huazhong University of Science and Technology, China, in 2006 and 2009, respectively.

He is currently a lecturer at the School of Electrical and Data Engineering, University of Technology Sydney (UTS), Australia. His current research interests include electrical machines and systems, multidisciplinary design optimization, industrial big data and cloud computing techniques.

Jianguo Zhu (S'93–M'96–SM'03) received the B.E. degree from Jiangsu Institute of Technology, China, in 1982, the M.E. degree from Shanghai University of Technology, China, in 1987, and the Ph.D. degree from the University of Technology, Sydney (UTS), Australia, in 1995, all in electrical engineering.

He is currently a professor of Electrical Engineering at the University of Sydney, Australia. His research interests include electromagnetics, magnetic properties of materials, electrical machines and drives, power electronics, and green energy systems.